Locally enhanced wintertime air-sea interaction and deep oceanic mixed layer formation associated with the subarctic front in the North Pacific

Hiroyuki Tomita,[1] Shinya Kouketsu,[1] Eitarou Oka,[2] and Masahisa Kubota[3]

Received 10 October 2011; revised 9 November 2011; accepted 10 November 2011; published 22 December 2011.

[1] Satellite-derived high-resolution air-sea flux data and Argo float data were analyzed to reveal the fine-scale spatial structures of air-sea turbulent heat and momentum fluxes and their relationship with the deep oceanic mixed layer around the subarctic front (SAF) in the North Pacific. An important feature inferred from the satellite-derived dataset is the presence of a pair of positive and negative air-sea flux anomaly bands with a width of 100–200 km on both sides of the SAF. Such a fine-scale structure in air-sea fluxes has not been captured in previous datasets. The SAF plays a significant role in determining the fine-scale structure of air-sea fluxes. The oceanic mixed layer is deeper to the south of the SAF, and the maximum mixed layer depth is observed near the positive anomaly band in air-sea fluxes. This study concludes that active air-sea interactions due to the presence of the SAF enhances upward air-sea heat and momentum fluxes to the south of SAF and selectively produces a deep oceanic mixed layer where the formation of Transition Region Mode Water occurs. **Citation:** Tomita, H., S. Kouketsu, E. Oka, and M. Kubota (2011), Locally enhanced wintertime air-sea interaction and deep oceanic mixed layer formation associated with the subarctic front in the North Pacific, *Geophys. Res. Lett.*, *38*, L24607, doi:10.1029/2011GL049902.

1. Introduction

[2] In the western North Pacific, the Kuroshio and Oyashio approach each other and then turn eastward as the Kuroshio and Oyashio Extensions, respectively [e.g., *Yasuda*, 2003]. The Kuroshio and Oyashio Extensions are associated with two major oceanic fronts in the upper ocean, namely, the Kuroshio Extension front (KEF) and the subarctic front (SAF), respectively. Such mid-latitude upper-oceanic fronts significantly influence the atmosphere through local air-sea interaction processes and the associated surface heat flux (HF) [*Xie*, 2004; *Small et al.*, 2008; *Minobe et al.*, 2008; *Kwon et al.*, 2010].

[3] The upper-oceanic fronts are also closely related to the development of deep oceanic mixed layers (MLs) in the winter, and thus, to the formation of mode waters [*Oka and Qiu*, 2011]. Using historical hydrographic data [*Suga et al.*, 2004] and Argo float observations [*Ohno et al.*, 2009], the presence of two distinct regions of deep winter MLs in the western North Pacific has been determined; these regions are associated with the KEF and SAF. One region of deep ML is centered at 32°N, 145–150°E to the south of the KEF and corresponds to the region of formation of the Subtropical Mode Water (STMW) [*Masuzawa*, 1969]. The other ML is centered at 42°N, 155–160°E to the southeast of the SAF and is considered to be the region of formation of the recently identified Transition Region Mode Water (TRMW) [*Saito et al.*, 2007].

[4] While the formation mechanism of the STMW has been thoroughly examined, that of the deep winter ML to the southeast of the SAF has not been studied in detail [*Oka and Qiu*, 2011]. Recently, the existence of a quasi-stationary jet along the SAF has been inferred from high-resolution sea surface temperature (SST) and current data obtained from satellite observations [*Isoguchi et al.*, 2006]. This jet is expected to transport warm and saline water from the south of the SAF to the surface layer in the region of formation of the TRMW. This results in an increase in the winter oceanic heat loss and surface water density, leading to the formation of the deep ML [*Saito et al.*, 2007]. However, it has not been determined whether a close relationship exists between the winter distribution of ML depth and the air-sea flux around the SAF; the inability to determine the relationship is probably because of the insufficient horizontal resolution of both the climatological ML data and the conventional air-sea flux data derived from atmospheric reanalysis.

[5] In order to better understand the influence of the SAF on the formation of the deep winter ML to its southeast, high-resolution air-sea flux data and in situ hydrographic observation data are indispensable. Recently, multisatellite observations with high spatial and temporal resolutions were used to obtain a new air-sea heat and momentum flux dataset known as the second version of the Japanese Ocean Flux Data Sets with Use of Remote Sensing Observations (J-OFURO2) [*Tomita et al.*, 2010; *Kubota et al.*, 2002]. This is a potentially powerful tool that can be used to describe the fine-scale structure of air-sea flux over frontal regions. In this paper, we analyze the high-resolution (0.25° × 0.25° grid) version of the J-OFURO2 air-sea flux dataset and Argo profiling float data to demonstrate the locally enhanced wintertime air–sea flux and deep ML formation associated with the SAF.

2. Results

[6] The location of the two major oceanic fronts, SAF and KEF, can be inferred from the winter SST and its southward gradient distributions (Figure 1). The SAF extends northeastward from 39°N, 146°E to 43°N, 158°E along almost the same route as that described by *Isoguchi et al.* [2006]. The

[1]Research Institute for Global Change, Japan Agency for Marine and Earth Science Technology, Yokosuka, Japan.
[2]Atmosphere and Ocean Research Institute, University of Tokyo, Kashiwa, Japan.
[3]School of Marine Science and Technology, Tokai University, Shimizu, Japan.

0094-8276/11/2011GL049902

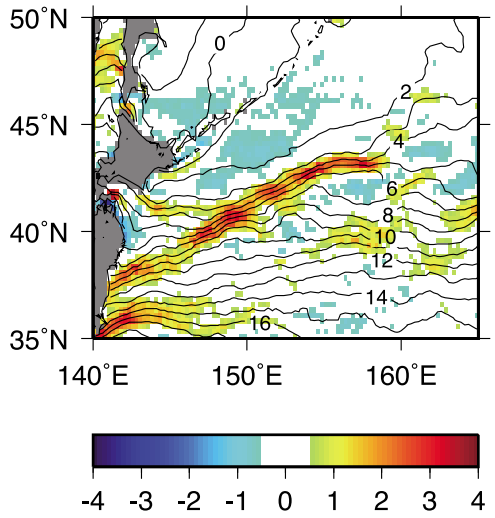

Figure 1. Spatial distribution of sea surface temperature (SST) (contour, °C) and its high-pass filtered southward gradient (color, °C/100 km) averaged over the period from January to April from 2002 to 2007 obtained using J-OFURO2 data.

KEF extends eastward from 35°N, 140°E, although it appears to be weak to the east of 146°E because of variation in its position [*Mizuno and White*, 1983; *Chen*, 2008]. The larger southward SST gradient along the SAF, compared with that along the KEF, reflects the quasi-stationary nature of the SAF [*Isoguchi et al.*, 2006].

[7] Turbulent winter air-sea fluxes, namely, sensible heat flux (SHF), latent heat flux (LHF), and momentum flux (MF), averaged over the period from January to April from 2002 to 2007, demonstrate the fine-scale spatial structure of the air-sea fluxes in the open North Pacific (Figure S1 in the auxiliary material).[1] Before temporal averaging, a spatial high-pass filter was applied to highlight variation at scales smaller than 1000 km (Figure 2). The obtained spatial pattern has not been clearly captured in previous datasets, including NCEP/NCAR reanalysis (Figures 2 and S1). Thus, J-OFURO2 is suitable for investigating mesoscale air-sea interaction in the vicinity of the SAF, which has spatial scales of <1000 km.

[8] An important feature detected from the J-OFURO2 data is a pair of positive and negative HF anomaly bands with a width of 100–200 km on both sides of the SAF. It is inferred that the SAF influences the air-sea HFs and enhances oceanic heat loss to the south of the front. The magnitude of the variation in the SHF is somewhat larger than that of the variation in the LHF. This contrasts with the results of previous studies on the air-sea HF around the KEF, where LHF is found to be larger than SHF [*Tokinaga et al.*, 2009].

[9] The cross-frontal variations in the turbulent heat flux (THF = SHF + LHF) anomaly and their contribution terms are shown in Figure 3a. The contribution terms were estimated by decomposing the bulk formula of HFs; this method has been applied in previous studies [e.g., *Tanimoto et al.*, 2003]. In our formulation, the THF anomaly from the cross-frontal meridional mean of unfiltered data is decomposed into contributions from the ocean (O), atmosphere (A), and surface wind (WND).

[1]Auxiliary materials are available in the HTML. doi:10.1029/2011GL049902.

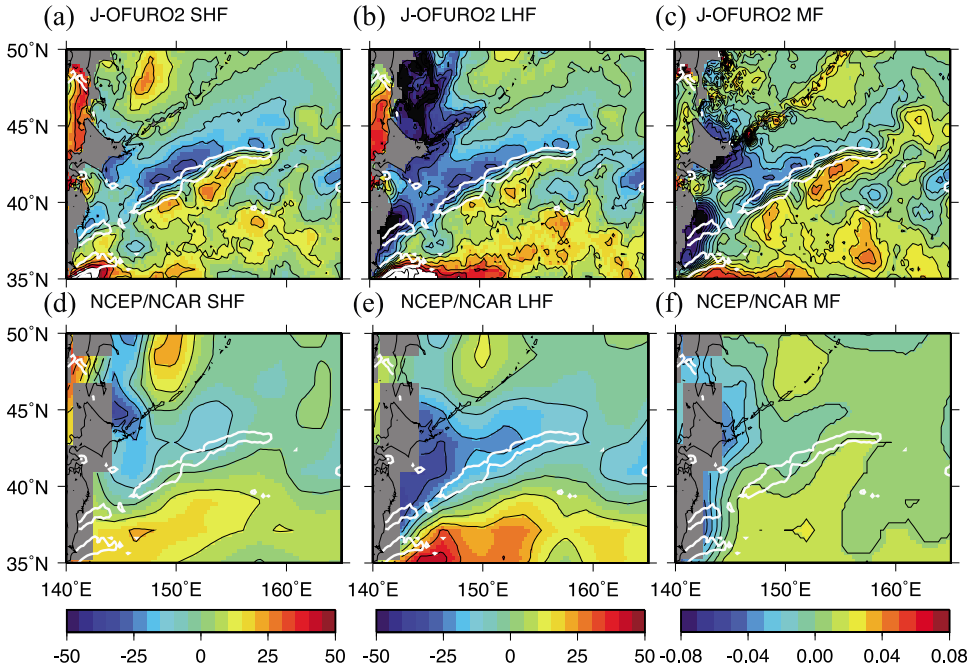

Figure 2. High-pass filtered spatial distributions (color and black contours) of the sensible heat flux (SHF), latent heat flux (LHF) (W/m^2; positive upward), and momentum flux (MF) (N/m^2) anomalies averaged over the period from January to April from 2002 to 2007 obtained using (a–c) J-OFURO2 and (d–f) NCEP/NCAR reanalysis. The contour intervals of the heat flux (HF) and MF anomalies are 10 W/m^2 and 0.01 N/m^2, respectively. High-pass filtered southward gradient of sea surface temperature (SST) obtained from J-OFURO2 was superimposed for the value of 1.5°C/100 km (white contour).

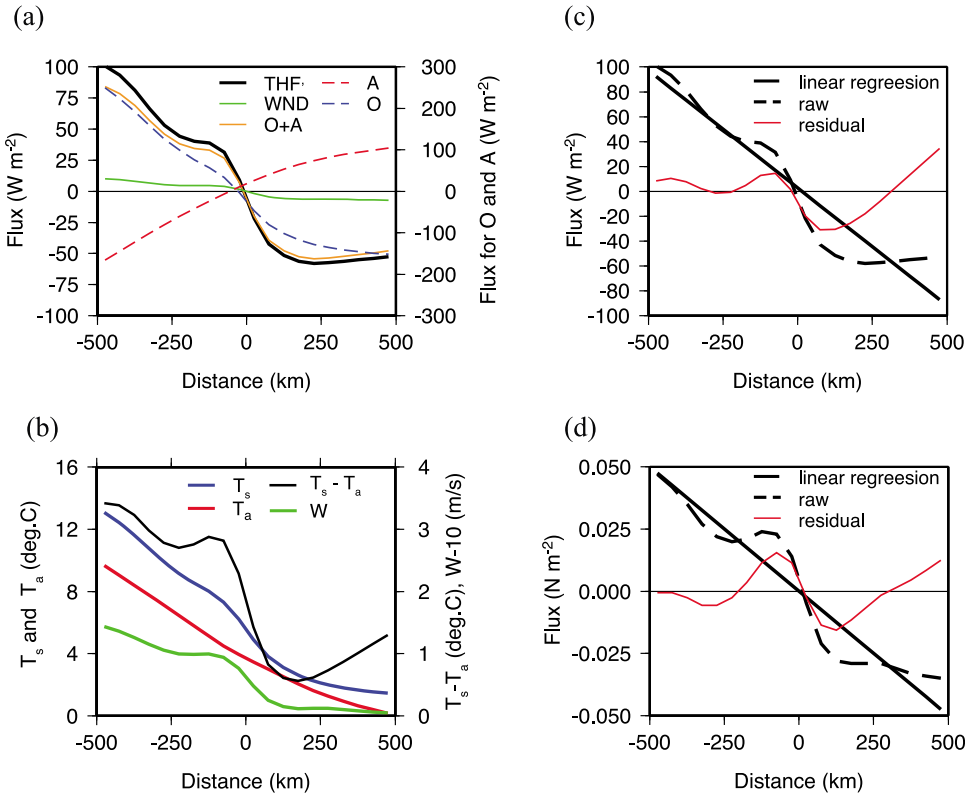

Figure 3. Composite cross-frontal sections of anomalous (a) turbulent heat flux and its contribution terms and (b) surface variables. (c and d) Anomalous turbulent heat and momentum fluxes with their regression and residuals. The fluxes are positive upward anomalies from the meridional mean. All values were averaged over the period from January to April from 2002 to 2007. The horizontal axis shows the distance (positive northward) relative to the subarctic front (SAF), whose location was defined as the maximum of the southward gradient of the high-pass filtered SST.

[10] The THF anomaly is positive (negative) to the south (north) of the SAF and changes sharply across the SAF (Figure 3a). This change in the THF anomaly is largely explained by the air-sea differences in temperature and humidity, shown as O + A in Figure 3a. Although the contribution of the surface wind speed to the THF anomalies is considerably smaller (<10 W/m^2) than that of the other terms, it tends to have the same sign as that of the THF anomalies. The influence of wind speed as a mechanical forcing mechanism on the upper ocean will be discussed later.

[11] To understand the physical mechanisms resulting in the cross-frontal variations and the local maximum of air-sea flux to the south of SAF, it is helpful to examine the nature of near-surface conditions. While both SST (T_s) and air temperature (T_a) increase from north to south as expected, across the SAF, the gradient of T_s is stronger than that of T_a; this causes the large air-sea temperature difference (T_s - T_a) to the south of the SAF (Figure 3b). This implies that across the SAF, T_a does not rapidly adjust to SST, and the northwesterly wind transports dry and cold air to the southeast of the SAF. Thus, the air-sea temperature difference has a local maximum to the south of SAF.

[12] To estimate the front-induced THF difference across the SAF, the THF anomaly was divided into two, namely, the anomaly arising from the influence of the large-scale meridional difference and that arising from the local influence of the SAF (Figure 3c); this was done under the assumption that by studying the linear regression field information regarding the large-scale field (without local oceanic front effect) can be obtained. The difference between THFs on both sides of the SAF at a distance of 75 km from the front (approximately 80 W/m^2) is much larger than that (approximately 40 W/m^2) calculated from the linear regression field of the THF across the front (Figure 3c). This suggests that the SAF could cause a meridional difference twice as large as one without the oceanic front.

[13] Surface wind speed (W) also changes significantly across the front, being 1 m/s larger to the south of SAF than to the north (Figure 3b). In addition, it exhibits a local maximum to the south of SAF corresponding to local maxima of THF and T_s - T_a. This is consistent with the vertical mixing mechanism proposed by *Wallace et al.* [1989] and supported by observations [*Nonaka and Xie*, 2003; *Tokinaga et al.*, 2006]. That is, enhanced THF activates vertical mixing in the atmospheric boundary layer to the south of the SAF, and, as a consequence, momentum is transported to the surface from the higher atmosphere. Although the cross-frontal changes in the wind speed do not have a remarkable influence on THF (<10 W/m^2), the influence of the SAF on MF is clear (Figure 3d). As in the case of the THF, the SAF is estimated to enhance meridional difference of momentum flux twice as large as one without the front.

[14] To investigate the influence of fine-scale air-sea fluxes on the upper ocean, the distribution of the winter oceanic ML around the SAF was examined; this distribution is based on

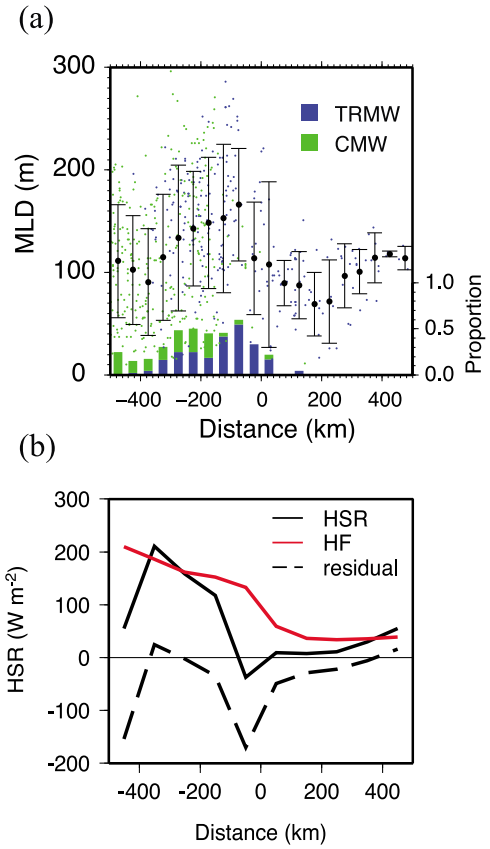

Figure 4. (a) Composite cross-frontal sections of oceanic mixed layer depth (small colored dots) in the period from January to April from 2002 to 2007. Large black dots and lines show the average and standard deviation for each bin of 50-km width. Colored bars indicate the proportion of the mixed layers deeper than 150 m to all mixed layers. (b) Composite cross-frontal sections of heat storage rate and its budget, averaged over January to April from 2002 to 2007.

the hydrographic data obtained by Argo profiling floats (Figure 4a). Here, ML depth was defined as the depth at which the potential density increases by 0.03 kg/m^3 from the value at the sea surface, following *de Boyer Montegut et al.* [2004]. The winter ML is much deeper on the southern side of the SAF than on the northern side, with a maximum depth reached approximately 50–100 km away from the SAF, where air-sea fluxes also reach their local maxima. This covariation suggests that mesoscale distribution of air-sea fluxes in association with the SAF has a significant influence on the layers in the surrounding upper ocean.

[15] To allow us to discuss the influence of air-sea fluxes quantitatively, the contribution of the HF to the upper ocean was estimated. For completeness, the contribution of the MF through the forcing of entrainment and other factors also needs to be quantified, but such a detailed analysis will be performed in a future study. Firstly, the thermal influence of surface HF on upper ocean temperature was evaluated. The temporal changes in heat storage between early winter (December to February) and late winter (March to May) were calculated from Argo temperature profiles of up to 300-m depth (hereafter, we refer to this as the heat storage rate, HSR; Figure 4b). A large amount of heat loss occurs in most part of the region to the south of SAF; the largest heat loss of 100–200 W/m^2 occurs at approximately 100–400 km distance from the SAF and little heat gain is observed near the front. On the other hand, to the north of the SAF, the HSR indicates small heat losses (<50 W/m^2). This suggests that the ocean requires heat loss of approximately 100–200 W/m^2 to produce the distribution of ML south of the SAF.

[16] To the south of the SAF, the heat loss by air-sea HF is approximately 150–200 W/m^2, which explains the HSR. Near the SAF heat loss by the air-sea HF greatly exceeds the HSR. The difference is probably caused by transport of warm water from the upstream region by the quasi-stationary jet [*Isoguchi et al.*, 2006].

[17] Locally deep MLs approximately 100 km south of the SAF mostly have salinities lower than 33.9 (Figure 4a), which are characteristic of the TRMW rather than the central mode water (CMW) [*Oka et al.*, 2011]. On the other hand, MLs approximately 200–300 km south of the SAF are characteristic of the CMW, which is characterized by more saline (>33.9) and warmer waters. This provides strong evidence that a deep ML constituting the source of the TRMW is locally formed south of the SAF.

3. Conclusion

[18] A satellite-derived high-resolution air-sea flux data set, J-OFURO2, and Argo profiling float data during the period from January to April from 2002 to 2007 have been analyzed to reveal the fine-scale structure of air-sea turbulent heat and momentum fluxes in winter and its relation to the formation of the deep oceanic ML around the SAF. An important feature detected by J-OFURO2 is a pair of positive and negative air-sea flux anomaly bands with a width of 100–200 km on both sides of the SAF. Such a fine-scale structure in air-sea fluxes has not been captured in previous datasets including the NCEP/NCAR reanalysis. The SAF plays a significant role in determining the fine-scale structure of air-sea fluxes. We concluded that the active air-sea interaction attributed to the existence of the SAF enhances the air–sea heat and momentum fluxes to the south of the SAF and selectively produces the deep MLs where the formation of TRMW occurs, as inferred by *Isoguchi et al.* [2006] and *Saito et al.* [2007].

[19] The mesoscale air-sea interaction and the production of deep oceanic ML revealed in this study and in preceding studies [*Uehara et al.*, 2003; *Itoh et al.*, 2011; *Kouketsu et al.*, 2011] have the potential to influence broader-scale ocean circulations and global climate through the variation in mode waters. Furthermore, the meridional migration of the SAF on decadal and interannual timescales [*Nonaka et al.*, 2006] can affect the processes. To further improve understanding, collaborative studies using both high-resolution satellite-derived air-sea HF data and Argo float data are important, and intensive and sustainable deploying of Argo floats in the world oceans, especially in the frontal regions, is essential.

[20] **Acknowledgments.** The authors thank Shinsuke Iwasaki for help in preparing the J-OFURO2. This research was supported in part by JAXA (Japan Aerospace eXploration Agency). The Argo float data used in this study were collected and made freely available by the International Argo Project and the national programs that contribute to it (http://www.argo.ucsd.edu, http://argo.jcommops.org). The author EO was supported in part by the Japan Society for the Promotion of Science [KAKENHI, Grant-in-Aid for Scientific Research (B) 21340133].

[21] The Editor thanks an anonymous reviewer for his or her assistance in evaluating this paper.

References

Chen, S. M. (2008), The Kuroshio Extension front from satellite sea surface temperature measurements, *J. Oceanogr.*, *64*, 891–897, doi:10.1007/s10872-008-0073-6.

de Boyer Montegut, C. D., G. Madec, A. S. Fischer, A. Lazar, and D. Iudicone (2004), Mixed layer depth over the global ocean: An examination of profile data and a profile-based climatology, *J. Geophys. Res.*, *109*, C12003, doi:10.1029/2004JC002378.

Isoguchi, O., H. Kawamura, and E. Oka (2006), Quasi-stationary jets transporting surface warm waters across the transition zone between the subtropical and the subarctic gyres in the North Pacific, *J. Geophys. Res.*, *111*, C10003, doi:10.1029/2005JC003402.

Itoh, S., Y. Shimizu, S. Ito, and I. Yasuda (2011), Evolution and decay of a warm-core ring within the western subarctic gyre of the North Pacific, as observed by profiling floats, *J. Oceanogr.*, *67*, 281–293, doi:10.1007/s10872-011-0027-2.

Kouketsu, S., H. Tomita, E. Oka, S. Hosoda, T. Kobayashi, and K. Sato (2011), The role of meso-scale eddies in mixed layer deepening and mode water formation in the western North Pacific, *J. Oceanogr.*, doi:10.1007/s10872-011-0049-9.

Kubota, M., N. Iwasaka, S. Kizu, M. Konda, and K. Kutsuwada (2002), Japanese ocean flux data sets with use of remote sensing observations (J-OFURO), *J. Oceanogr.*, *58*, 213–225, doi:10.1023/A:1015845321836.

Kwon, Y. O., M. A. Alexander, N. A. Bond, C. Frankignoul, H. Nakamura, B. Qiu, and L. Thompson (2010), Role of the Gulf Stream and Kuroshio-Oyashio systems in large-scale atmosphere–ocean interaction: A review, *J. Clim.*, *23*, 3249–3281, doi:10.1175/2010JCLI3343.1.

Masuzawa, J. (1969), Subtropical Mode Water, *Deep Sea Res.*, *16*, 463–472.

Minobe, S., A. Kuwano-Yoshida, N. Komori, S. P. Xie, and R. J. Small (2008), Influence of the Gulf Stream on the troposphere, *Nature*, *452*, 206–209, doi:10.1038/nature06690.

Mizuno, K., and W. B. White (1983), Annual and interannual variability in the Kuroshio Current System, *J. Phys. Oceanogr.*, *13*, 1847–1867, doi:10.1175/1520-0485(1983)013<1847:AAIVIT>2.0.CO;2.

Nonaka, M., and S. P. Xie (2003), Covariations of sea surface temperature and wind over the Kuroshio and its extension: Evidence for ocean-to-atmosphere feedback, *J. Clim.*, *16*, 1404–1413, doi:10.1175/1520-0442(2003)16<1404:COSSTA>2.0.CO;2.

Nonaka, M., H. Nakamura, Y. Tanimoto, T. Kagimoto, and H. Sasaki (2006), Decadal variability in the Kuroshio-Oyashio Extension simulated in an eddy-resolving OGCM, *J. Clim.*, *19*, 1970–1989, doi:10.1175/JCLI3793.1.

Ohno, Y., N. Iwasaka, F. Kobashi, and Y. Sato (2009), Mixed layer depth climatology of the North Pacific based on Argo observations, *J. Oceanogr.*, *65*, 1–16, doi:10.1007/s10872-009-0001-4.

Oka, E., and B. Qiu (2011), Progress of North Pacific mode water research in the past decade, *J. Oceanogr.*, doi:10.1007/s10872-011-0032-5.

Oka, E., S. Kouketsu, K. Toyama, K. Uehara, T. Kobayashi, S. Hosoda, and T. Suga (2011), Formation and subduction of Central Mode Water based on profiling float data, 2003–08, *J. Phys. Oceanogr.*, *41*, 113–129, doi:10.1175/2010JPO4419.1.

Saito, H., T. Suga, K. Hanawa, and T. Watanabe (2007), New type of pycnostad in the western subtropical-subarctic transition region of the North Pacific: Transition region mode water, *J. Oceanogr.*, *63*, 589–600, doi:10.1007/s10872-007-0052-3.

Small, R. J., S. P. deSzoeke, S. P. Xie, L. O'Neill, H. Seo, Q. Song, P. Cornillon, M. Spall, and S. Minobe (2008), Air-sea interaction over ocean fronts and eddies, *Dyn. Atmos. Oceans*, *45*, 274–319, doi:10.1016/j.dynatmoce.2008.01.001.

Suga, T., K. Motoki, Y. Aoki, and A. M. Macdonald (2004), The North Pacific climatology of winter mixed layer and mode waters, *J. Phys. Oceanogr.*, *34*, 3–22, doi:10.1175/1520-0485(2004)034<0003:TNPCOW>2.0.CO;2.

Tanimoto, Y., H. Nakamura, T. Kagimoto, and S. Yamane (2003), An active role of extratropical sea surface temperature anomalies in determining anomalous turbulent heat flux, *J. Geophys. Res.*, *108*(C10), 3304, doi:10.1029/2002JC001750.

Tokinaga, H., Y. Tanimoto, M. Nonaka, B. Taguchi, T. Fukamachi, S. P. Xie, H. Nakamura, T. Watanabe, and I. Yasuda (2006), Atmospheric sounding over the winter Kuroshio Extension: Effect of surface stability on atmospheric boundary layer structure, *Geophys. Res. Lett.*, *33*, L04703, doi:10.1029/2005GL025102.

Tokinaga, H., Y. Tanimoto, S. P. Xie, T. Sampe, H. Tomita, and H. Ichikawa (2009), Ocean frontal effects on the vertical development of clouds over the western North Pacific: In situ and satellite observations, *J. Clim.*, *22*, 4241–4260, doi:10.1175/2009JCLI2763.1.

Tomita, H., M. Kubota, M. F. Cronin, S. Iwasaki, M. Konda, and H. Ichikawa (2010), An assessment of surface heat fluxes from J-OFURO2 at the KEO and JKEO sites, *J. Geophys. Res.*, *115*, C03018, doi:10.1029/2009JC005545.

Uehara, H., T. Suga, K. Hanawa, and N. Shikama (2003), A role of eddies in formation and transport of North Pacific Subtropical mode water, *Geophys. Res. Lett.*, *30*(13), 1705, doi:10.1029/2003GL017542.

Wallace, J. M., T. P. Mitchell, and C. Deser (1989), The influence of sea-surface temperature on surface wind in the eastern equatorial Pacific: Seasonal and interannual variability, *J. Clim.*, *2*, 1492–1499, doi:10.1175/1520-0442(1989)002<1492:TIOSST>2.0.CO;2.

Xie, S. P. (2004), Satellite observations of cool ocean–atmosphere interaction, *Bull. Am. Meteorol. Soc.*, *85*, 195–208, doi:10.1175/BAMS-85-2-195.

Yasuda, I. (2003), Hydrographic structure and variability in the Kuroshio-Oyashio Transition Area, *J. Oceanogr.*, *59*, 389–402, doi:10.1023/A:1025580313836.

S. Kouketsu and H. Tomita, Research Institute for Global Change, Japan Agency for Marine and Earth Science Technology, Yokosuka, Kanagawa 237-0061, Japan. (tomitah@jamstec.go.jp)

M. Kubota, School of Marine Science and Technology, Tokai University, Shimizu, Shizuoka 424-8610, Japan.

E. Oka, Atmosphere and Ocean Research Institute, University of Tokyo, Kashiwa, Chiba 277-8564, Japan.